TRIGGER DISCHARGES AND PHOTOELECTRON PRODUCTION AT ENGINEERING SURFACES

E.M. Williams*

1. INTRODUCTION

An essential part in the switching action of a spark gap is the generation of electrons to initiate the current pulse. These electrons may be produced photoelectrically using radiation from a subsidiary discharge which is provided at the instant of switching. Forms of discharges are, for example, the corona around conductors of small radius, a spark discharge or, as has been used previously in the fast beam-extraction system at the CERN proton synchrotron [1], a discharge initiated across the surface of a dielectric of high permittivity. The dielectric serves to intensify the field strength at the regions of dielectric-metal interface, and measurements have confirmed the usefulness of this arrangement as a trigger discharge with low breakdown threshold and low ($\lesssim$ 1ns) time jitter [2]. The present report describes an investigation of the efficiency with which radiation from a trigger discharge of this kind can generate photoelectrons. The work was motivated by the extensive use being made of spark gaps in the fast beam-extraction facility currently being prepared in the FES Group for the 78 GeV proton synchrotron in Serpukhov, U.S.S.R., with the desire to check the aspect of photoelectron production in these spark gaps.

* Permanent address: Dept. of Electrical Engineering and Electronics, The University, P.O. Box 147, Liverpool L69.3BX, England.

The trigger discharge as shown schematically in Figure 1 consists of a tungsten rod 1 mm in diameter housed in a tube of aluminium-oxide ceramic which, in turn, fits in a brass former. For the purpose of the present tests, the trigger source was incorporated in a metal chamber provided with a quartz window through which radiation from the discharge passed to the exterior. The chamber could be pressurised up to 5 atm, and the dried air used in the tests could be vented through at a controlled rate. The discharge was initiated by a negative pulse of peak amplitude around 20 kV (5-95 % rise time $\sim$ 8 ns, RC fall time $\sim$ 100 ns) applied to the tungsten rod. The impulse was derived from a 50 ohm source, and with breakdown at the trigger pin the 50 ohm resistor between the brass former and ground provided a matched load. The efficiency of production of photoelectrons by radiation from the discharge was investigated using an auxiliary ionization chamber stressed at a potential below the breakdown potential. The arrangement is illustrated in Figure 1. Anode and cathode of the ionization chamber were in the form of discs of diameter 1 cm and made of brass. Radiation admitted into the ionization chamber via a quartz window passed to the cathode through a central hole of diameter 0.5 cm in the anode. In this way, a flash from the trigger source produces a pulse of, say, n_o photoelectrons which, in turn, give rise to an electron avalanche of magnitude $n = n_o \exp(\alpha d)$ in the ionization chamber, α being the primary ionization coefficient and d the interelectrode spacing. The size of the avalanche is clearly proportional to the number of photoelectrons induced by the light flash, and this forms the basis of the present experimental technique.

The electron avalanches were detected electrically by measuring the potential developed by the charge carriers across a resistor placed in series with the anode, and an analysis of the electrical circuit together with a discussion of some considerations in applying the proposed technique are presented below.

2. SOME CONSIDERATION IN APPLYING THE PROPOSED TECHNIQUE

In proposing this experiment, it must be borne in mind that the phenomenon of ionization is a statistical process, so that the size of electron avalanches even at a fixed number of starting electrons will exhibit some fluctuations. The extent of these fluctuations will depend on the number of starting electrons and on the value of the primary ionization coefficient α. In the case of avalanches initiated by single electrons the distribution in size is generally quite broad and is given according to: [3]

$$q(n) = \frac{1}{\bar{n}} \exp\left(\frac{-n}{\bar{n}}\right) \qquad (1)$$

where $q(n)$ represents the probability of finding an avalanche of size n, and $\bar{n}$ is the mean avalanche size given according to $n = \exp(\alpha d)$. Of course, with increasing number of starting electrons, these statistical effects become of less importance, and calculations indicate that in the region above ten starting electrons the statistical effects are largely ruled out [4]. It is of special interest to draw attention to the result (1) since an examination of the distribution of avalanche sizes provides a method of determining α, and a knowledge of this coefficient is required to make use of the proposed method in a quantitative manner.

For convenient measurement of electron avalanches, the amplification provided in the ionization chamber should be as high as possible. However, not so high that secondary processes of ionization or space charge influence come into play since they would introduce a more linear relation between $\bar{n}$ and n_o. In the present work the ionization chamber was operated in room air (pressure 730 torr, temperature 22°C) and the interelectrode spacing could be set between the limits 0-10 mm. Under these conditions of pressure and spacing the maximum amplification that can be attained before breakdown occurs is $10^5 - 10^6$, so that working a few per cent of

voltage below the static breakdown the amplification would be expected to be $\sim 10^4$. This corresponds to a total electron charge $\sim 10^{-15}$ coulomb per initiatory electron.

The electrical circuit for the measurements is shown in Figure 2a, where r and c represent respectively the resistor placed in series with the anode and the parasitic capacity from anode to ground. An amplifier of input resistance r_a and input capacity c_a is shown connected across r. This whole arrangement can be represented as shown in Figure 2b where resistance and capacity have been combined in parallel with $C = c+c_a$ and $R = \frac{r\, r_a}{r+r_a}$. The relationship between the carrier current I_c and the voltage V at the input of the amplifier is:

$$I_c = \frac{V}{R} + C \frac{dV}{dt} . \qquad (2)$$

If the value of the product RC is very much greater than the time scale of carrier motion, considering now both electrons and the much slower positive ions, then the voltage across the resistor is obtained as the integral of the current. The peak value is attained in a time τ_+, corresponding to the positive ion transit time between the electrodes, and is given by [5]:

$$V = \frac{n_o e}{C} \exp(\alpha d). \qquad (3)$$

For time greater than τ_+ the signal decays as $e^{-t/RC}$.

On the other hand, if the value of the product RC is very much less than the time scale of carrier development, the displacement term in equation (2) may be neglected and $V = I_c R$ with [5]:

$$I_c = \frac{n_o e\, v_-}{d} \exp(\alpha v_- t) , \qquad (4)$$

where v_- is the electron drift velocity. The integrating circuit provides the most convenient and sensitive manner of measuring the total charge contained in an avalanche, but the direct method was also of interest in order to gain some insight into the growth mechanism.

3. PRELIMINARY INVESTIGATIONS

Two amplifier systems were made use of for observing the electrical signals at the anode of the ionization chamber: one, a Keithley model 104 wideband amplifier with input resistance 1 meg-ohm and input capacity 10 pF. The other, a Tektronix probe type 010-130 of input resistance 10 meg-ohm and input capacity 7 pF, used in conjunction with a type 82 plug-in. The parasitic capacity from the anode of the ionization chamber to ground was 13 pF, yielding values of total capacity C of 23 and 20 pF.

The conditionschosen to operate the ionization chamber are listed in Table 1, form which it may be noted that the interelectrode spacing was set as 4 mm with a negative voltage of 12.5 kV applied to the cathode. This voltage was some 300 V below the static breakdown limit. Also listed in Table 1 are the values of transport and ionization coefficients appropriate to the chosen conditions, as deduced from published data [5,6,7] and also confirmed by experiments performed in the course of this work. The growth of electron avalanches proceeds in time as $\exp(\alpha v_- t)$, so that to make direct observations of avalanche growth $RC \ll 1/\alpha v_- \ll 4$ ns. This condition is difficult to fulfill, also it is difficult to meet the requirements of the rise time of the amplifier. The smallest RC investigated in this work was in the region 10 ns, obtained using the Keithley model 104 amplifier in conjunction with a load resistor ~ 500 ohm (the rise time of the amplifier was some 3 ns). Typical oscillograms obtained in this way are shown in Figure 3 in which the initial build up of electron current lasting some 40 ns is clearly identifiable. With the

TABLE 1

Conditions in the Ionization Chamber
and Data on Transport and Ionization Coefficients

Gas pressure	$p = 730$ torr at 22°C
Gas spacing	$d = 0.4$ cm
Applied voltage	$V = 12.5$ kV
Breakdown voltage	$V_s = 12.8$ kV
Ratio of field strength to gas pressure	$E/p = 43$ V cm^{-1} torr^{-1}
Electron drift velocity	$v_- = 10^7$ cm sec^{-1}
Electron transit time	$\tau_- = 40$ ns
Positive ion drift velocity	$v_+ = 10^5$ cm s^{-1}
Positive ion transit time	$\tau_+ = 4$ µs
Primary ionization coefficient	$\alpha = 25$ cm^{-1}

limitations of the measuring system for direct observation, the decay of the electron pulse would be expected to be elongated to some 40 ns. However, from the figure it can be seen that an aftercurrent persists for some 4-5 µs. This time is of the order of the positive ion transit time τ_+, and yet the aftercurrent is far too strong to be identified with positive ions (the positive ion current is smaller than the electron current by the ratio v_+/v_- of the positive ion to electron drift velocity, i.e. $\sim 10^{-2}$). Similar oscillograms have been observed by the Hamburg school in air and in other electronegative gases [5], and the aftercurrent is attributed to the formation of negative ions with the subsequent detachment of electrons to yield free electrons late in the discharge *. The oscillograms leave little

* More recent studies of swarms in electronegative gases show that oscillograms of this kind do not necessarily imply a detachment reaction, but can be explained on the basis of the motion of electrons and (stable) negative ions. I am indebted to Professor J.D. Craggs for pointing this out.

doubt as to the presence of negative ions, but it may be noted that no structure is in evidence to suggest that any secondary ionization process is active (with processes of electron attachment the primary ionization coefficient α should, strictly speaking, be replaced by α' where $\alpha' = \alpha - \eta$, η being the attachment coefficient. For the present purpose, however, the notion of α will be retained although the α written in this way really refers to α').

The condition to obtain an integrated signal of the carrier current is $RC \gg 1/\alpha v_+ \gg 400$ ns. This criterion could readily be satisfied using either amplifier system with the input impedance of the amplifier providing the resistive load. The probe unit provided sensitivities in excess of 10 mV/cm on the oscilloscope screen while the Keithley amplifier provided for sensitivities in the range 200 μV-500 mV/cm. Typical oscillograms obtained in these conditions are shown in Figure 4. The current grows during the initial 5 μs, corresponding to the positive ion transit time, and subsequently decays with a time constant $\sim$ 200 μs in agreement with expectations. The peak height of the signal represents the total charge divided by the value of capacity C (following eqn (3)), and to deduce the number of electrons which initiated the avalanche there remains the value of α to be determined.

A knowledge of α is equivalent to a knowledge of the average signal from an avalanche initiated by one electron. The distribution in size with single electron avalanches is given by equation (1) and the value of α was determined by applying this result to measurements of the distribution in size of single electron avalanches. Conditions of predominantly single electron avalanches were arranged by removing the trigger discharge to a large distance from the ionization cell when avalanche signals were seen in only about 40 % of the cases in which the trigger discharge was operated. Measurements were carried out in a relatively crude fashion by simply counting on the oscilloscope screen the frequency of occurrence at three series of limits of

magnitude. The sensitivity setting for the measurement was equivalent to 400 μV/cm of the oscilloscope screen which may be compared with a predicted mean signal ~ 100 μV if the amplification in the ionization chamber is $\sim 10^4$. Results obtained in this way are shown in Figure 5 plotted as the logarithm of frequency of occurrence versus the number of electrons contained in the avalanche. The three measurements are seen to lie close to a straight line, and the slope of the line yields $\bar{n} = 2.8 \times 10^4$. This yields $\alpha d = 10$, or $\alpha = 25\ cm^{-1}$ which may be compared with the value $\alpha = 22\ cm^{-1}$ derived from data published by Von Engel [7], and with the result $\alpha d = 9.6$ measured by Frommhold [8] at a setting some 50 volts below the static breakdown limit in air at pressure p = 500 torr with distance d = 2 cm. The result $\bar{n} = 2.8 \times 10^4$ corresponds to an average signal of 0.2 mV from an avalanche initiated by one electron.

4. EXAMINATION OF PHOTOELECTRON PRODUCTION

Photoelectron production was first investigated as a function of the spacing between the trigger discharge and the ionization chamber, and the results of measurements of the integrated electrical signal as a function of spacing are shown in Figure 6 plotted on a log-log scale. Two series of measurements are included, one with pressure 1 atm and the other with pressure 3 atm in the trigger housing. In either case, the trigger discharge was excited by an impulse of peak amplitude 20 kV, and each point shown in the figure represents an average value of integrated signal obtained by superimposing 100 consecutive shots on a photographic plate, or by direct visual observation over 100 shots. The data obtained for each pressure are seen to lie on straight lines with gradients of close proximity; for the case of 1 atm, the derived dependence of signal on spacing is as $(\text{spacing})^{-5.8}$. This result is very different from an inverse square dependence and is indicative of absorption of the radiation in air. The signals obtained at the higher pressure of 3 atm lie consistently above the corresponding signals at 1 atm and the results of measurements aimed

to show this pressure dependence in greater detail are illustrated in Figure 7. The measurements were obtained at a spacing of 10.5 cm for trigger voltages of 20 and 25 kV. At a given trigger voltage the signal is seen to increase continually with increasing pressure. A dependence of the signal on setting of trigger voltage is also apparent, and some tests made with 3 atm pressure in the trigger housing indicated a linear rate of increase over the range of trigger voltages from 5 to 25 kV.

The signals shown in Figure 6 range from around 2 to 1000 mV which in view of the calibration described in § 3 correspond to numbers of photoelectrons in the range 10 to 5000 - the scale of number of starting electrons is included in Figure 6. In the spark gaps of the Serpukhov project, the trigger discharge illuminates a cathode of annular form with the trigger pin arranged in line with the axis of the annulus as depicted in Figure 8. The distances between the trigger discharge and cathode are in the range 2 to 4 cm, with the line joining the centre of the trigger discharge to the cathode surface making angles of respectively 65 and 75° with the normal to the cathode surface. The measurements presented in Fig. 6 were limited to a minimum separation between trigger discharge and ionization chamber of some 8 cm, however, with the linear form of response obtained by plotting the data on a log-log scale it is quite convenient to extrapolate to smaller values of separation. Data obtained in this way for separation of 2 and 4 cm are presented in Table II.

TABLE II

Extrapolated data of Fig. 6

Separation cm	Pressure 1 atm		Pressure 3 atm	
	Signal mV	N° of starting electrons	Signal mV	N° of starting electrons
2	2.2×10^6	1.1×10^7	1.8×10^6	9×10^6
4	4×10^4	2×10^5	5×10^4	2.5×10^5

The results indicate the photoelectron production to be largely independent of gas pressure in the trigger housing, and extracting the mean of the data the number of starting electrons is given as 10^7 at 2 cm and 2.25×10^5 at 4 cm. It may be noted that these figures refer, firstly, to electron production from a circular area of cathode as defined by the projection on to the cathode of the line joining the centre of the trigger discharge to the edges of the hole in the anode, and, secondly, to the situation in which the source of radiation is arranged in line with the normal to the cathode surface drawn at the centre of the area of cathode under illumination. Taking into account these geometric factors the number of starting electrons in the case of the spark gap of the Serpukhov project is calculated as 1.3×10^7 per cm^2 at the innermost region of the annular cathode (separation 2 cm) and 2.3×10^5 per cm^2 at the outermost surface of the cathode (separation 4 cm). This estimate is based on the assumption that the light output from the trigger discharge is isotropic and to check this point experiments were conducted with the trigger discharge rotated with respect to the ionization chamber. At 3 atm pressure in the trigger housing the isotropy was investigated over the range 0 to 40^c, but with the front of the trigger housing removed, and hence 1 atm pressure, measurements were possible over the more extensive range of 0 to 80°. In either case, no indications were observed to suggest a preferential direction of light emission.

The measurements which have been discussed so far were obtained with a brass cathode, whereas the material used as electrode material in the spark gaps was one of two tungsten alloys. Furthermore, the polished state of the brass cathode was in direct contrast to the heavily pitted condition of the surface of an electrode when in use in the spark gaps. It was therefore of considerable interest to investigate photoelectron production from the same tungsten alloys as used in the spark gap and, moreover, to employ cathodes with surfaces which were characteristic of the condition of the spark gap

electrodes. The tungsten alloys were, firstly, a material containing 75 % tungsten, 22 % copper with the remainder largely iron, and, secondly, an alloy containing 95 % tungsten with $\sim$ 5 % iron. Tests were made using both these materials and the surface preparation was as follows: in the case of the 75 % tungsten alloy, the surface was lightly tarnished by some low-energy sparks, whereas the cathode made of the material containing 95 % tungsten was cut from an actual electrode which had been in use in the spark gaps - the surface, thus, was heavily cratered. The results of measurements of the integrated signal height versus the separation between discharge source and ionization chamber as obtained with these materials are compared with the data obtained with the brass cathode in Figure 9. Notwithstanding the differences in materials and surface conditions the three sets of measurements are seen to lie close to each other; there is perhaps a tendency for the data obtained with the cathode of 75 % tungsten to lie a little higher, but this difference is within the margin of uncertainty in resetting conditions in the ionization chamber. The results thus indicate the photoelectron production to be invariant to the choice of cathode material and also independent of the surface condition at the cathode.

5. CONCLUSIONS AND DISCUSSION

Photoelectron production using the trigger source is generally quite efficient. The estimates of production in the case of the spark gap of the Serpukhov project are 1.3×10^7 per cm^2 at spacing between trigger discharge and cathode of 2 cm and 2.3×10^5 per cm^2 at spacing of 4 cm. These figures are based on relatively large extrapolations, but it may be noted that with no quartz whatsoever between trigger source and ionization chamber there was a tendency for the signal at smaller separations ($\lesssim$ 10 cm) to increase at a rate greater than that depicted in Figure 6. On this basis, the estimates should be considered as being quite conservative.

However, in assessing the estimates it must be borne in mind that they represent the photoelectron production integrated over the period of excitation of the trigger discharge. This was borne out by the results of some direct observations of electron motion made with high levels of signal which showed the rise time of the electron current to be elongated beyond the customary 40 ns to around 160 ns. Clearly, an advancement of this work would be to study the temporal evolution of photoelectrons.

The intensity of the radiation emitted from the trigger discharge increases with increasing height of the trigger pulse and also with increasing gas pressure. The radiation is quite strongly absorbed in air in such a way that the overall result for cathodes spaced 2 - 4 cm from the trigger discharge is that the production of photoelectrons is largely independent of gas pressure. If the attenuation of radiation is described according to the customary law $I(x) = I_0 \exp(-Ax)$, where A is the absorption coefficient and x is the distance traversed beyond the point where the intensity is I_0, then the decrement in signal in going from 2 to 4 cm in the case of unit atm pressure (allowing for the decrease in solid angle) corresponds to a value of absorption coefficient of 1.2 cm^{-1}. If a similar calculation is extended to larger separation between cathode and trigger source, following the data presented in Figure 6, values of absorption coefficient (corresponding to unit atm pressure) are found of smaller magnitude and lying in the range 0.5 to 0.03 cm^{-1}. This conforms with a picture whereby the frequency components of the radiation that are most strongly absorbed in air are filtered out in the initial few cm, with the less strongly absorbed components penetrating to larger distances. The value for absorption coefficient ~ 1 cm^{-1} clearly lays stress on the importance of distance consideration in designing a spark gap.

The production of photoelectrons was found to be independent of the constituents and of the surface condition of the cathode. The materials used as cathodes in these tests were most certainly covered with oxide layers, and as such the results refer to photo-electron production from oxide layers rather than from clean metallic substrates. The inactivity of the role of the cathode is in keeping with the general trends observed in gas discharge studies conducted with cathodes of similar character [9].

In conclusion, a few remarks may be pertinent as to the nature of the radiation produced at the trigger discharge which stimulates electron emission. The radiation was largely unaffected by quartz glass, yet with a piece of ordinary window glass placed between the trigger discharge and the ionization chamber all avalanche activity ceased. Quartz has a cut-off at wavelengths less than 0.18 μm [10], and ordinary glass at wave lengths less than about 0.35 μm. The observations thus imply a wavelength of the radiation in the range 0.18 - 0.35 μm. This result is in keeping with the conclusion drawn by comparing the measured values of absorption co-efficient with published data on the specular absorption coefficient in air [10] which, for an absorption coefficient ~ 1 cm^{-1}, implies a wavelength ~ 0.185 μm. It is interesting to note the strong absorp-tion of ultra-violet radiation by ozone gas which is the main action in filtering solar ultra-violet radiation in the earth's atmosphere. An appreciable amount of ozone gas is produced by running an electrical discharge in air, and for this reason the absorption of ultra-violet in a spark gap could be even more severe than the present measurements indicate. This stresses the need for adequate replenishment of the air supply to a spark gap.

6. ACKNOWLEDGEMENTS

It is a pleasure to acknowledge the encouragement of Dr. B. Kuiper in this work. This work was carried out during a period of two months as visiting scientist at CERN, and the author wishes to thank the members of the FES Group who provided technical assistance.

7. REFERENCES

1. L. Caris and E.M. Williams, CERN 69-13 (1969).

2. J.K.M. Verbist, CERN Internal Report PS/FES/TN-273 (1971).

3. W. Legler, Z. Phys., 140, 221 (1955).

4. W.T. McArthur and D.J. Tedford, Proc. Int. Conf. on Gas Discharges, I.E.E. Pub. N° 70, 284 (1970).

5. H. Raether: "Electron Avalanches and Breakdown in Gases", (London: Butterworths) (1964).

6. L. Frommhold, Z. Phys., 160, 554 (1960).

7. A. von Engel: "Ionized Gases" (Oxford: Clarendon Press) (1965).

8. L. Frommhold, Z. Phys., 150, 172 (1958).

9. C. Grey Morgan: "Fundamentals of Electric Discharges in Gases", (Oxford: Pergamon Press) (1966).
J.M. Meek and J.D. Craggs: "Electrical Breakdown of Gases", (Oxford: Clarendon Press) (1953).

10. M. von Ardenne: "Tabellen der Electronenphysik, Ionenphysik und Ubermikroskopie" (Berlin: Veb Deutscher Verlag Der Wissenschaften) (1956).

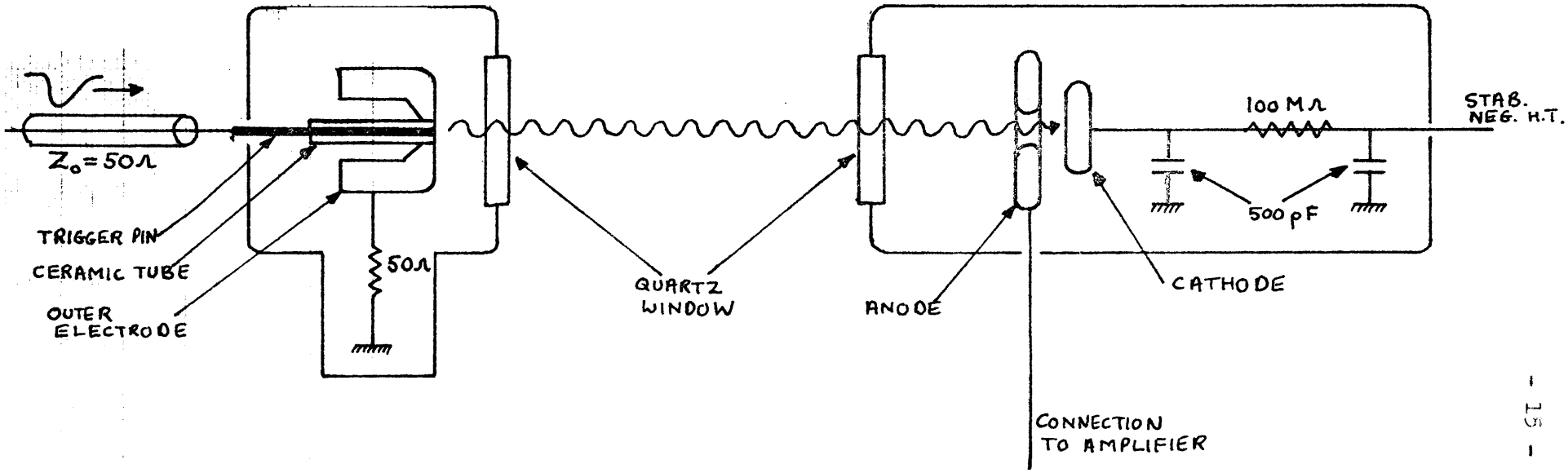

Fig.1 SCHEMATIC REPRESENTATION OF THE EQUIPMENT

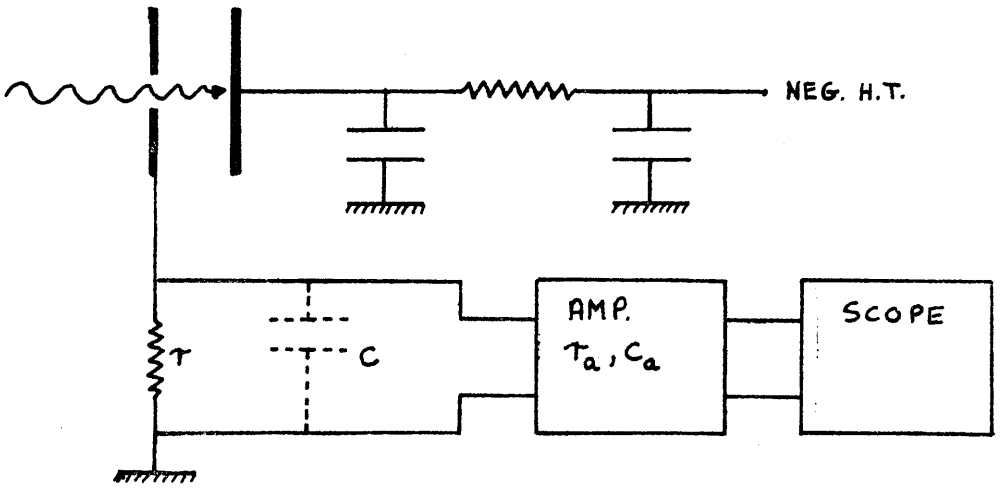

(a)

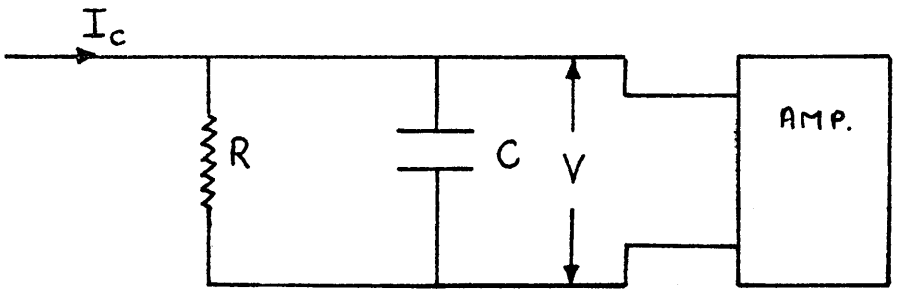

(b)

Fig. 2 (a) THE ELECTRIC CIRCUIT, and (b) THE EQUIVALENT REPRESENTATION.

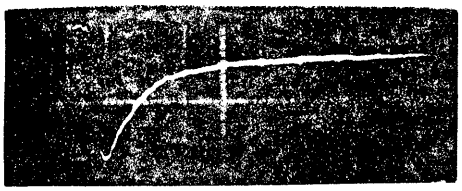

100 ns/division

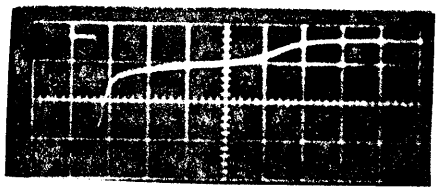

1 μs/division

Fig. 3 DIRECT OBSERVATIONS OF CARRIER MOTION

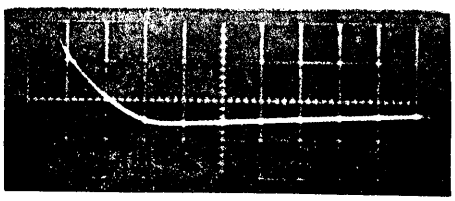

2 μs/division

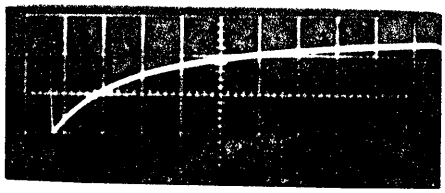

50 μs/division

Fig. 4 OBSERVATIONS OF INTEGRATED CURRENT

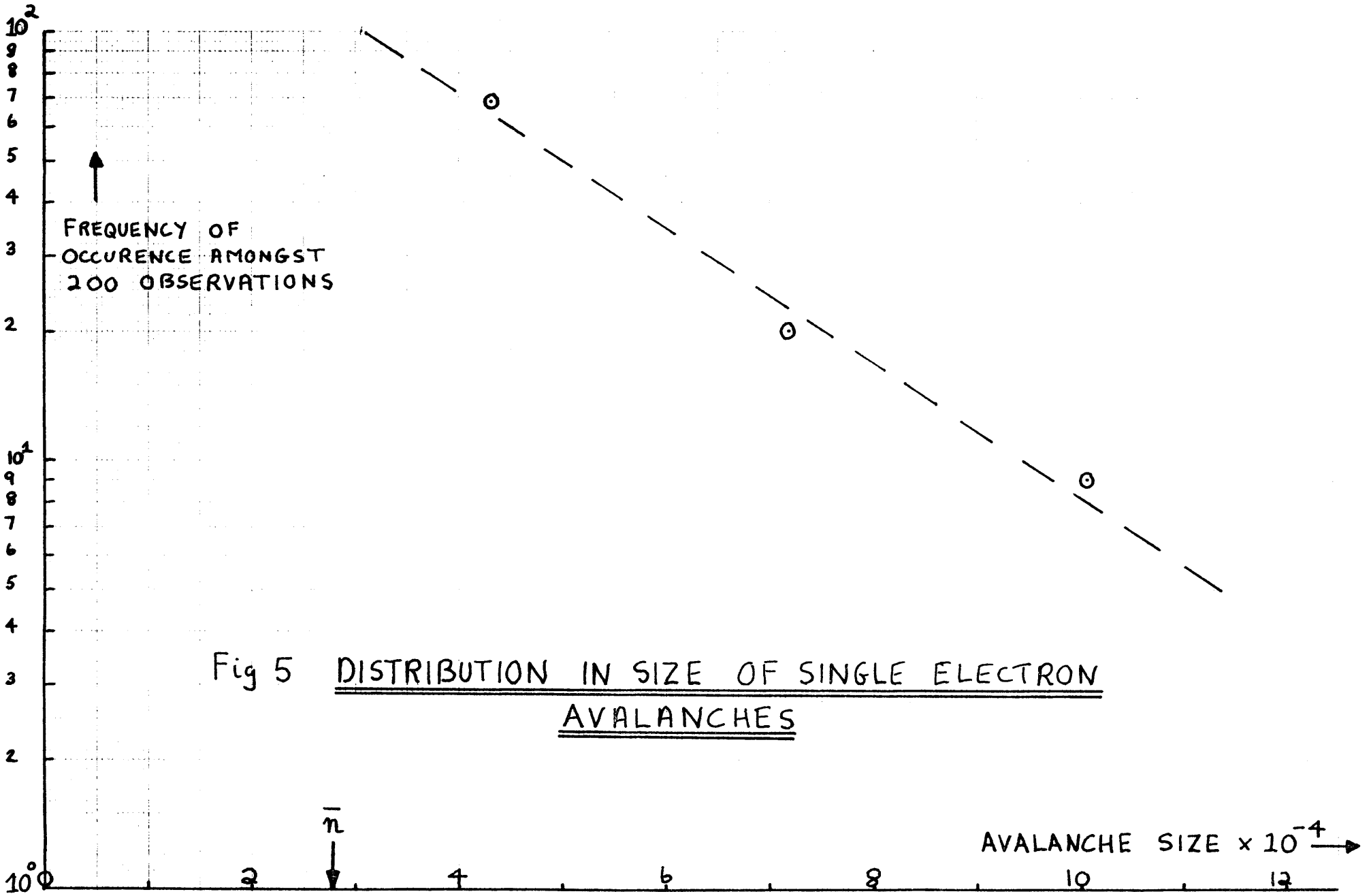

Fig 5 DISTRIBUTION IN SIZE OF SINGLE ELECTRON AVALANCHES

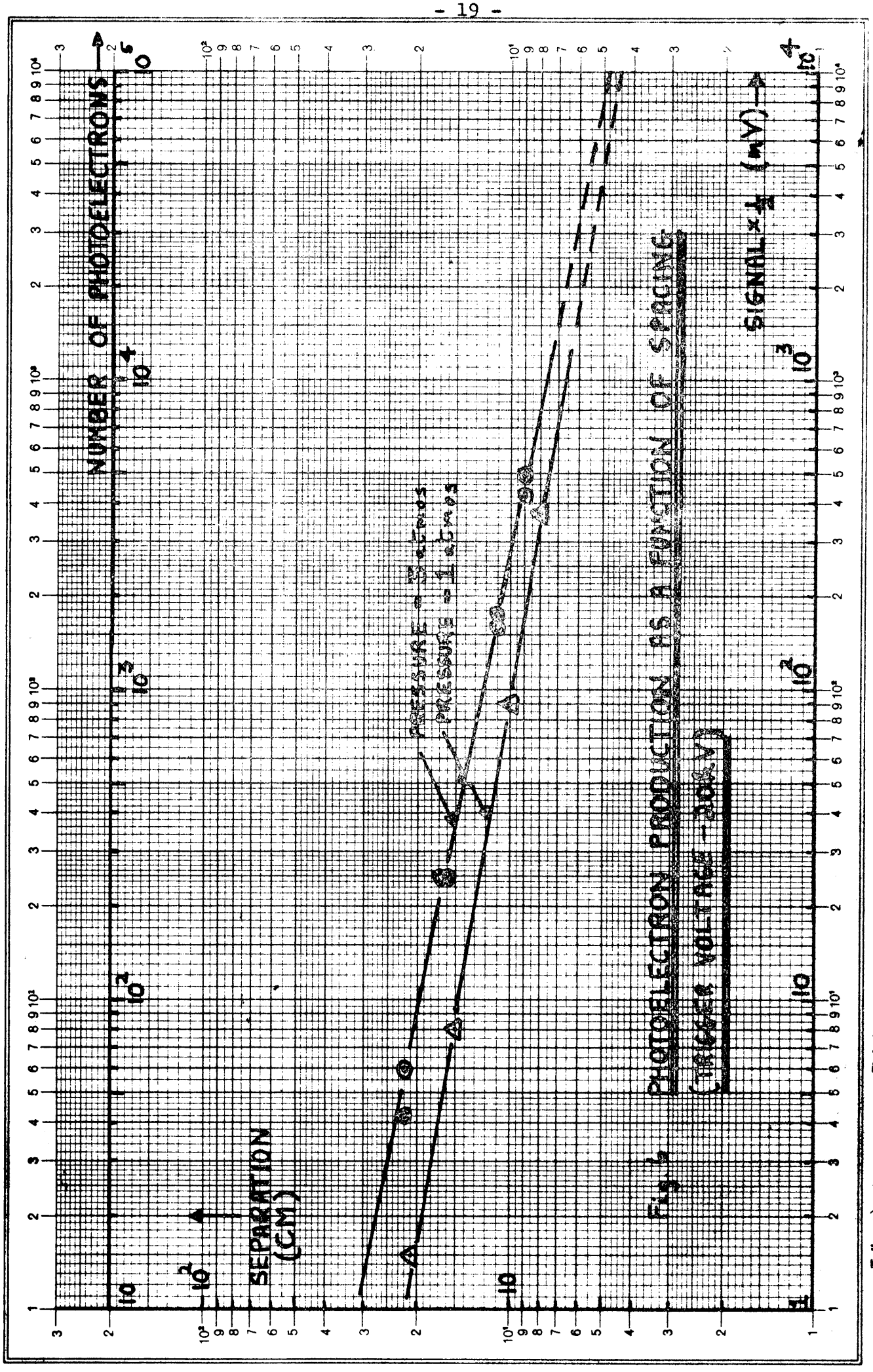

Fig. 4 PHOTOELECTRON PRODUCTION AS A FUNCTION OF SPACING (SURFACE VOLTAGE = 20 kV)

Logar. Teilung 1-300 u. 1-10000 Einheit 62,5 mm
Logar. Division Unité
Ed. Aerni-Leuch, Bern, Nr. 551

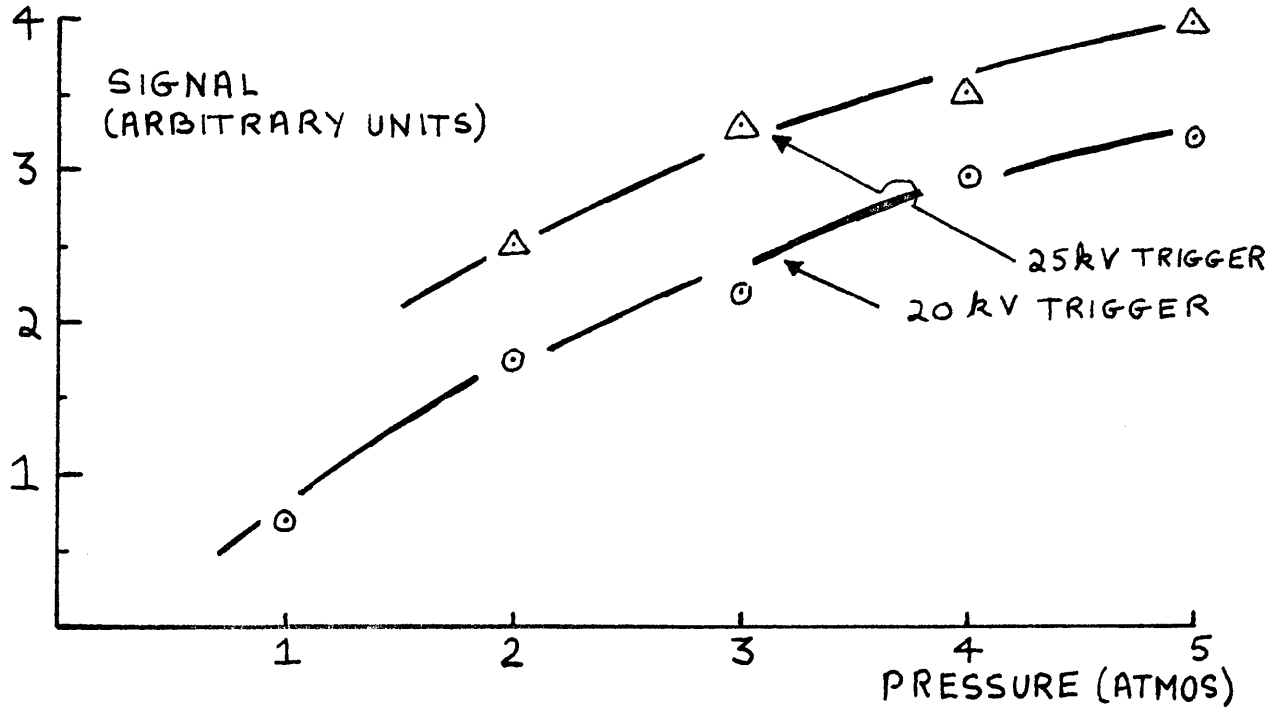

Fig. 7 DEPENDENCE OF PHOTOELECTRON PRODUCTION ON GAS PRESSURE

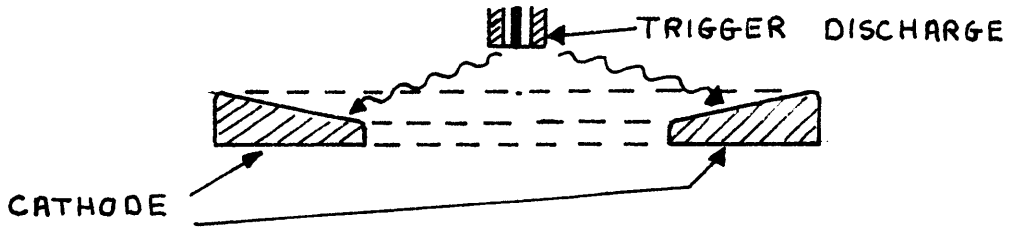

Fig. 8 ARRANGEMENT OF TRIGGER DISCHARGE AND FIRST CATHODE IN THE SPARK GAP

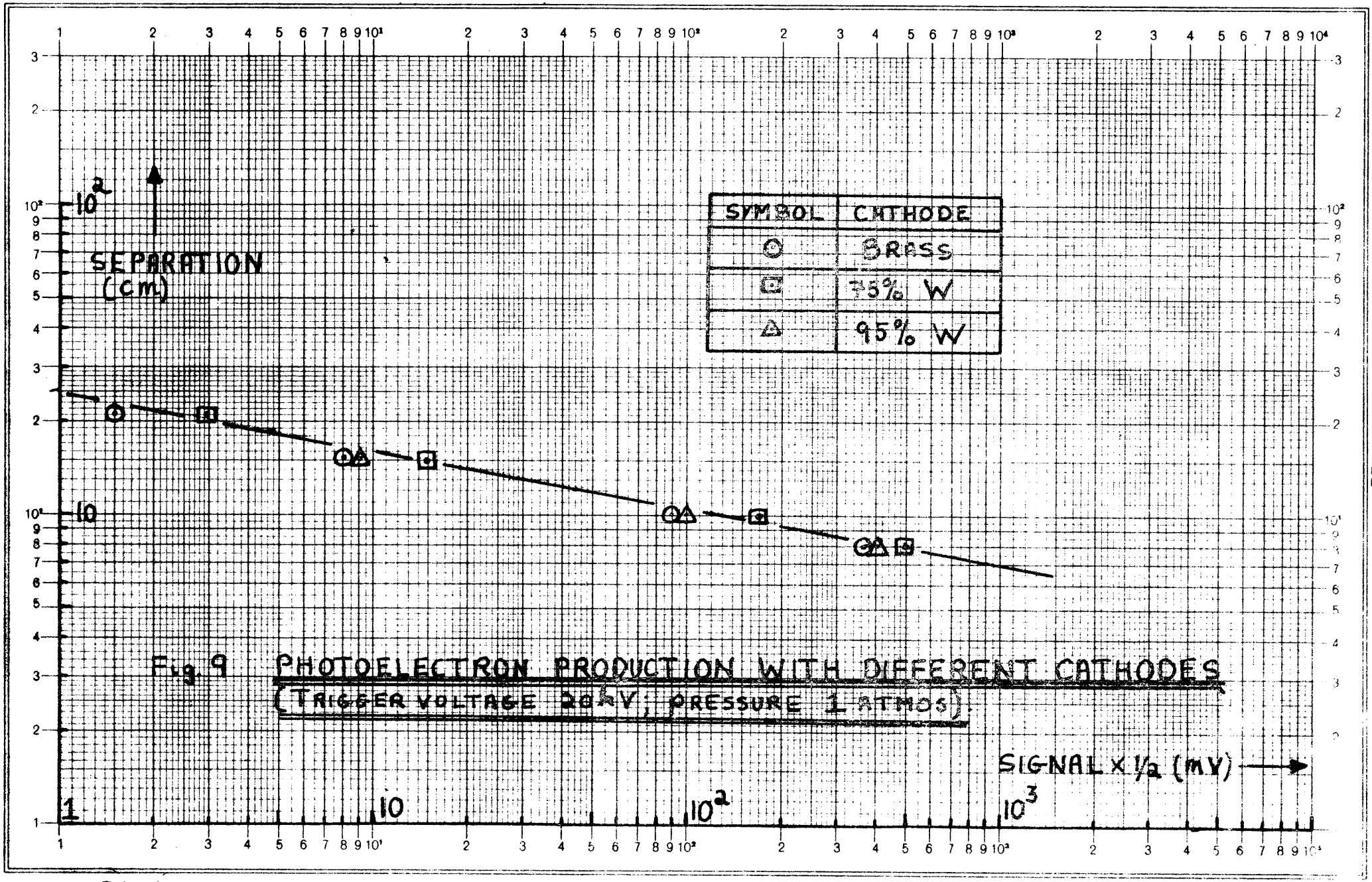

Fig. 9 PHOTOELECTRON PRODUCTION WITH DIFFERENT CATHODES
(TRIGGER VOLTAGE 20 kV; PRESSURE 1 ATMOS)

Logar. Teilung / Division 1-300 u. 1-10000 Einheit / Unité 62,5 mm

Ed. Aerni-Leuch, Bern, Nr. 551